Laser Phase Noise Tolerant and Power-Fading-Free Hybrid Fiber-Wireless Double-Sideband Transmission With Spectral Efficiency Enhancement

Jiankang Li , Yuancheng Cai , *Member, IEEE*, Shitong Xiang, Xiaoguang Yang, Mingzheng Lei , *Member, IEEE*, Bingchang Hua , *Member, IEEE*, Jiao Zhang , *Member, IEEE*, Junjie Ding , *Member, IEEE*, Yucong Zou , Xingyu Chen , Xiang Liu , Yunwu Wang , Jianjun Yu , *Fellow, IEEE*, and Min Zhu , *Member, IEEE*

Abstract—The photonics-assisted millimeter-wave (MMW) communication technology is attractive to facilitate the MMW application in the upcoming B5G and 6G networks. However, its generated MMW signal by optical heterodyne detection usually suffers from serious laser phase noise, which will severely deteriorate the system performance. In this paper, based on a single dual-drive Mach-Zehnder modulator and a single-end photodetector, we first present a simple and spectrally efficient hybrid fiber-wireless double-sideband transmission by employing an overlapping frequency multiplexing scheme. That is, two independent wireless signals with an identical carrier frequency can be simultaneously transmitted in the hybrid fiber-wireless links. To recover the above two overlapped signals, and cancel the concomitant laser phase noise at the same time, a novel digital signal processing method for carrier extraction and signal recovery is further proposed. A proof-of-concept experiment using two independent 3-GBd quadrature phase shift keying (QPSK) signals at W band (92.5 GHz) is performed. After up to 80-km fiber and 3-m wireless transmission, the two QPSK signals can be successfully demodulated, without using the traditional carrier phase estimation algorithm. The proposed scheme not only can double the spectral efficiency of conventional double sideband transmission scheme, but also is immune to its power fading phenomenon induced by chromatic dispersion and robust to the laser phase noise resulting from two free-running lasers in the photonics-assisted MMW communication link.

Index Terms—Overlapping frequency multiplexing, laser phase noise, double-sideband transmission, power fading, spectral efficiency, fiber-wireless access.

Jiankang Li, Shitong Xiang, Xiaoguang Yang, Xiang Liu, and Yunwu Wang are with the National Mobile Communications Research Laboratory, Southeast University, Nanjing 210096, China (e-mail: jkangli0921@seu.edu.cn; stxiang@seu.edu.cn; 220221171@seu.edu.cn; xiangliu@seu.edu.cn; wangyunw@seu.edu.cn).

Yuancheng Cai, Jiao Zhang, and Min Zhu are with the National Mobile Communications Research Laboratory, Southeast University, Nanjing 210096, China, and also with the Purple Mountain Laboratories, Nanjing 211111, China (e-mail: caiyuancheng@pmlabs.com.cn; jiaozhang@seu.edu.cn; minzhu@seu.edu.cn).

Mingzheng Lei, Bingchang Hua, Junjie Ding, Yucong Zou, and Xingyu Chen are with the Purple Mountain Laboratories, Nanjing 211111, China (e-mail: 2016010326@bupt.cn; huabingchang@pmlabs.com.cn; dingjunjie@pmlabs.com.cn; zouyucong@pmlabs.com.cn; chenxingyu@pmlabs.com.cn).

Jianjun Yu is with the Purple Mountain Laboratories, Nanjing 211111, China, and also with Fudan University, Shanghai 200433, China (e-mail: jianjun@fudan.edu.cn).

Digital Object Identifier 10.1109/JPHOT.2024.3415354

I. INTRODUCTION

THE rapid proliferation of bandwidth-intensive applications has led to a significant surge in the demand for bandwidth in wireless communication systems. Consequently, there is an urgent need to expand the wireless communication spectrum from low-frequency microwave frequencies (such as sub-6 GHz) to high-frequency millimeter-wave (MMW) (30∼300 GHz). The latter can provide dozens of times of license-free spectrum resources as compared with the former, benefiting from the intrinsic large available bandwidth of MMW band. In order to promote MMW application in the upcoming B5G and 6G networks, the photonics-assisted MMW communication technology is a promising solution. This technology can not only generate MMW signal in a low-cost and tunable manner, but also greatly expend the coverage area by integrating the flexible wireless access with the advantages of ultra-low-loss fiber transmission [1], [2], [3]. However, the generated MMW signal in the photonics-assisted MMW communication link usually suffers from serious laser phase noise, which mainly results from the heterodyne detection of two free-running lasers [4]. Therefore, exploring the simple and low-cost phase noise cancellation method is a critical issue worth studying. On the other hand, compared with other transmission schemes, the double-sideband (DSB) scheme has lower requirements on the system structure/device, and can significantly simplify the system cost and power consumption. However, the low spectral efficiency of DSB signal and the problem of power fading induced by chromatic dispersion hinder its wide application.

Generally speaking, to improve the spectral efficiency of the system, in addition to using vector high-order modulation formats, the most common way is adopting the polarization

division multiplexing (PDM) scheme. Two independent wireless signals can be simultaneously transported over an optical and MMW carrier through a pair of orthogonal polarization directions. This is apparently different from the traditional subcarrier multiplexing (SCM) scheme, in which independent wireless signals are carried by different electrical carriers to avoid the spectrum overlap before being modulated on a single optical carrier [5], [6], [7]. For the PDM scheme, two independent wireless signals can be simultaneously transmitted with different [8], [9], [10] or identical carrier frequencies [11], [12]. The latter can provide a higher spectral efficiency by making full use of the limited spectrum resources. Meanwhile, the antenna polarization multiplexing technique, which employs a pair of dual-polarized antennas [13], [14] instead of commonly used 2×2 multiple-input multiple-output separate antennas [15], [16], can also realize the high spectral efficiency transmission of MMW signals in the wireless channels.

In recent years, a new approach termed as the overlapping frequency multiplexing (OFM) scheme for radio-over-fiber links can also modulate multiple signals on a single optical/wireless carrier. Since two or more independent signals share the same spectrum resources, this OFM scheme can enhance the spectral efficiency over both optical fiber and wireless links, even for the DSB transmission scheme. Moreover, it should be emphasized that the OFM scheme does not conflict with the PDM and SCM schemes mentioned above, which means that the spectral efficiency of the system can be further improved by their joint cooperation. Some previous works have verified the feasibility of the OFM scheme in typical microwave photonic links [17], [18], [19], [20], [21]. Using a dual-parallel Mach-Zehnder modulator (MZM) consisting of three MZMs [17], or the cascade of an intensity modulator and a phase modulator [18], two independent microwave vector signals carried by an identical carrier frequency at about 2 GHz can be successfully modulated and demodulated over a single optical carrier. However, these works rely on one or more expensive transceiver components to realize the modulation and detection of two independent microwave vector signals, which inevitably increases the system costs. Moreover, in order to cancel the phase noise originating from coherent detection, a self-coherent optical local oscillator (LO) is delivered from the optical transmitter to the receiver. It occupies one polarization state different from the signal lightwave, thus the potential capacity of these systems will be halved due to the loss of PDM signal transmission capability. To overcome the above shortcomings, a simplified transmitter based on the dual-drive MZM (DDMZM) for simultaneous modulation of two independent microwave vector signals on a single polarization in [19] or four on the dual polarizations in [20] has also been successfully demonstrated. Unfortunately, an expensive optical coherence receiver consisting of one 90° optical hybrid and four single-end photodiodes (PDs) is required for signal detection at each polarization. This is inconsistent with the typical structure of photonics-assisted MMW communication systems which prefers to use simple optical heterodyne detection based on one single-end PD per polarization [22]. In addition, although the dominant laser phase noise has been cancelled by the unique signal demodulation digital signal processing (DSP),

the above systems may still suffer from the residual phase noise due to path mismatch or phase imbalance between the in-phase and quadrature ports of the optical coherence receiver [23].

In this paper, an OFM scheme enabled by a simple DDMZM and a low-cost single-end PD has been presented and successfully demonstrated in the photonics-assisted MMW communication system. Two independent 3-GBd quadrature phase shift keying (QPSK) DSB signals with an identical carrier frequency are simultaneously transmitted over up to 80-km standard single-mode fiber (SSMF) and 3-m wireless at the W band (i.e., 92.5 GHz) for the first time. A novel DSP approach based on the RF pilot tone (RFP) technique [24], [25] is also proposed, which can successfully recover the two independent QPSK signals, meanwhile cancel the phase noise from the two free-running lasers during optical heterodyne detection. Since the transmitted signals only go through one single optical/wireless path, the residual phase noise due to path mismatch can be avoided in this system. Besides, the proposed DSP approach is also immune to the power fading of the DSB signal, which is induced by the fiber chromatic dispersion (CD). As compared with the conventional DSB scheme under the same transmission bandwidth, our proposed scheme can achieve a double transmission rate. The contrast between our proposed scheme and other OFM schemes is shown in Table I. It can be seen that our proposed OFM transmission scheme supports phase noise robustness with a simpler system configuration, thus it is more suitable for the future photonics-assisted MMW communication systems.

This paper is organized as follows. Section II first presents the operation principle of the proposed photonics-assisted MMW communication link using OFM transmission. The experimental setup and the corresponding result discussions are then shown in Sections III and IV, respectively. Finally, Section V concludes this paper.

II. PRINCIPLE

A. System Structure for OFM Transmission

The schematic diagram of the proposed photonics-assisted MMW communication link with OFM transmission based on single DDMZM modulation and single-end PD detection is shown in Fig. 1. Two independent microwave vector signals are first generated in the transmitting DSP. Assume that the two independent microwave vector signals, $s_1(t)$ and $s_2(t)$, are given as

$$s_1(t) = I_1(t)\cos(2\pi f_s) + Q_1(t)\sin(2\pi f_s) \quad (1)$$

$$s_2(t) = I_2(t)\cos(2\pi f_s) + Q_2(t)\sin(2\pi f_s) \quad (2)$$

where $I_1(t)$ and $I_2(t)$, $Q_1(t)$ and $Q_2(t)$ are the real and imaginary parts of two independent complex baseband signals, respectively. The two independent microwave vector signals exhibit an overlapping spectrum with the same center frequency of f_s.

To avoid power imbalance during the electro-optic modulation, the two signals are first cross-processed by $u_1(t) = s_2(t) + s_1(t)$ and $u_2(t) = s_2(t) - s_1(t)$, then they are modulated by a low-cost DDMZM. By biasing the DDMZM at its quadrature transmission point, the optical orthogonal modulation can be

TABLE I
SUMMARY OF PREVIOUS MICROWAVE/MMW PHOTONICS LINKS USING OFM SCHEME

Reference	Carrier frequency	Optical transmitter	Optical/wireless receiver[a]	Receiving DSP	Phase noise robustness	Support signal PDM
[17]	2 GHz	DP-MZM[b]	2 BPDs[c] & 2 ADCs[d]	Simple	Yes	No
[18]	2.5 GHz	MZM & PM[e]	2 BPDs & 2 ADCs	Middle	Yes	No
[19]	4 GHz	DDMZM	2 BPDs & 2 ADCs	Complex	Yes	Yes
[20]	4 GHz	DP-DDMZM[f]	2 BPDs & 2 ADCs	Complex	Yes	Yes
[21]	2.5 GHz	MZM & PM	2 BPDs & 2 ADCs	Middle	Yes	Yes
This paper	92.5 GHz	DDMZM	1 single-end PD & 1 ADC	Middle	Yes	Yes

[a]Note: Only single polarization is considered for fair comparison; [b]DP-MZM: dual-parallel Mach–Zehnder modulator; [c]BPD: balanced photodetector consisting of 2 single-end PDs; [d]ADC: analog-to-digital converter; [e]PM: phase modulator; [f]DP-DDMZM: dual-polarization dual-drive Mach-Zehnder modulator.
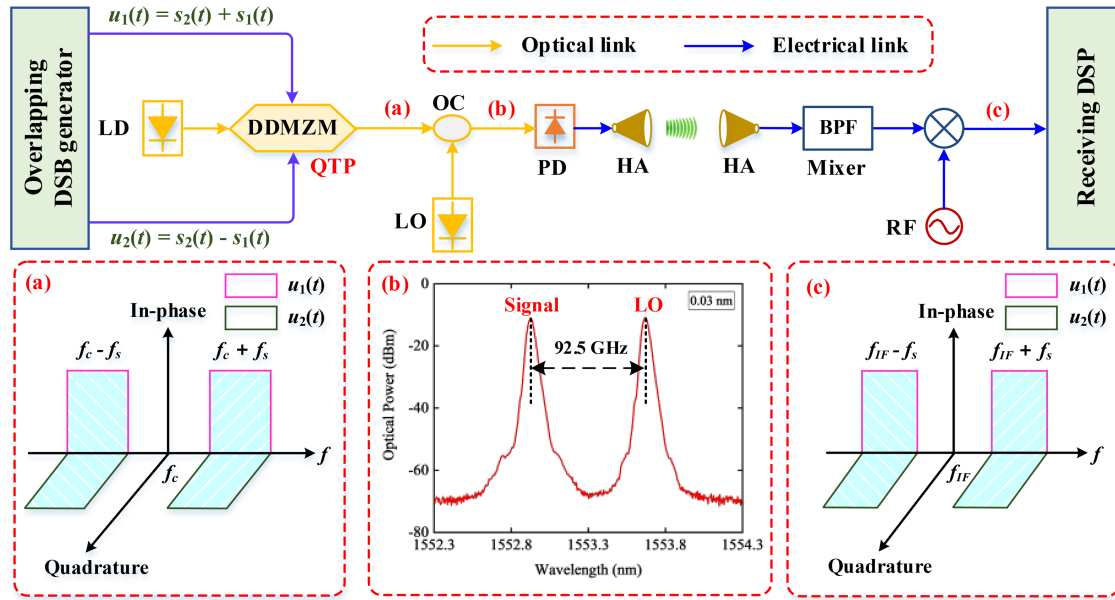

Fig. 1. Schematic diagram of the proposed photonics-assisted MMW communication link with OFM transmission based on single DDMZM modulation and single-end PD detection. OFM, overlapping frequency multiplexing; LD, laser diode; DDMZM, dual-drive Mach-Zehnder modulator; QTP, quadrature transmission point; OC, optical coupler; LO, local oscillator; PD, photodiode; HA, horn antenna; RF, radio frequency; IF, intermediate frequency; DSP, digital signal process.

achieved, whose output signal can be expressed as [26]

$$E_s(t) = \frac{\sqrt{2}}{2} E_c(t) \cdot \left[\exp\left(jm \cdot u_1(t) - jm \cdot \frac{V_\pi}{2} \right) + \exp\left(jm \cdot u_2(t) \right) \right] \quad (3)$$

where $m = \pi/V_\pi$ represents the modulation depth and V_π is the half-wave voltage of the DDMZM. $E_c(t)$ denotes the unmodulated lightwave generated by a laser diode (LD). Assume the LD is expressed as $E_C(t) = \sqrt{P_C}\exp[j2\pi f_C t + \varphi_C(t)]$, P_C, f_C and $\varphi_C(t)$ are the optical power, central frequency and phase noise of the LD, respectively. The modulated optical OFM signals after DDMZM can be approximated as $u_1(t) + j \cdot u_2(t)$ under small signal driving condition [27], the corresponding spectra are shown in the inset (a) of Fig. 1. It can be seen that the OFM signals with two overlapping DSB are orthogonal to each other in the phase domain. This orthogonality originates from the optical orthogonal modulation of DDMZM, and it acts as a key role to realize the demodulation of two overlapping DSB signals

at the receiver end, which will be introduced in the following. Although at first glance, this orthogonal modulation used in this paper seems similar to the IQ modulation realized by using the IQMZM or DDMZM [28], [29], the signal transmission form, DSP processing flow, and how to achieve the robustness to laser phase noise and immunity to power fading have apparent differences.

After coupled with a LO lightwave, the combined optical signals are fed to a single-end PD for optic-electro detection. Assume the LO is expressed as $E_{LO}(t) = \sqrt{P_{LO}}\exp[j2\pi f_{LO}t + \varphi_{LO}(t)]$, P_{LO}, f_{LO} and $\varphi_{LO}(t)$ are the optical power, central frequency and phase noise of the LO, respectively. The optical spectra of the combined optical signals before the PD are shown in inset (b) of Fig. 1. Then the desired MMW signal can be generated by optical heterodyne detection, its center frequency equals to the frequency difference between the two lightwaves. The output signal of PD can be expressed as

$$I_{PD}(t) = R \cdot |E_s(t) + E_{LO}(t)|^2$$
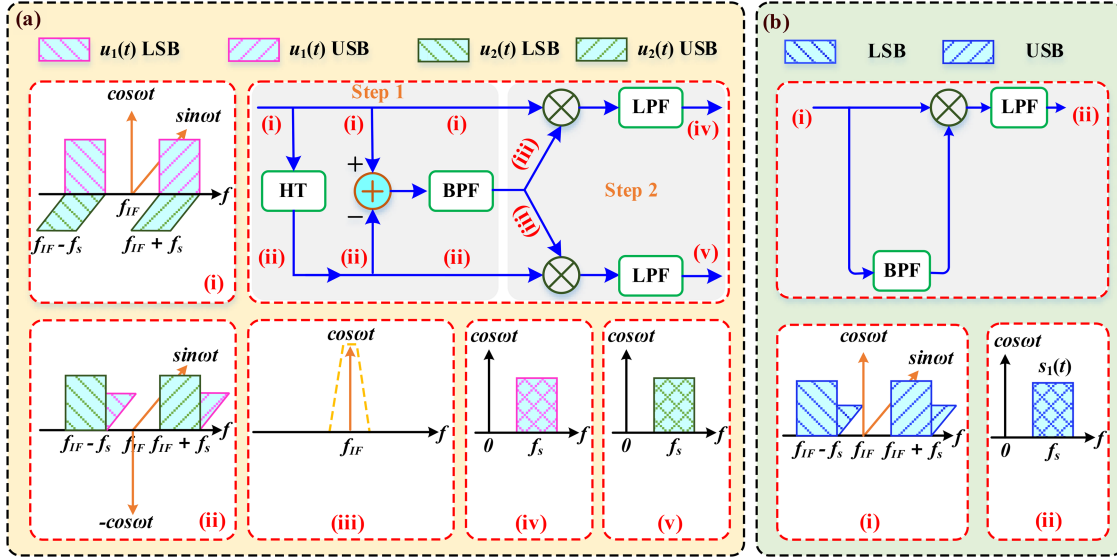$$= R(P_c + P_{LO}) + RP_c \cdot \sin[m(u_1(t) - u_2(t))]$$

Fig. 2. (a) Proposed carrier extraction and signal recovery DSP approach for OFM transmission with two overlapping DSB signals. (b) Conventional RFP phase noise cancellation scheme for one single DSB signal. HT, Hilbert transform; BPF, band-pass filter; LPF, low-pass filter; LSB, lower side-band; USB, upper side-band.

$$+ R\sqrt{P_C P_{LO}} \cdot [\sin(2\pi f_{RF} t + \varphi_{RF}(t) + mu_1(t))$$
$$+ \cos(2\pi f_{RF} t + \varphi_{RF}(t) + mu_2(t))] \qquad (4)$$

Where R is the responsivity of the PD, P_C is the optical power of the optical wave at the output of the LD, $f_{RF} = f_c - f_{LO}$ and $\varphi_{RF}(t) = \varphi_c(t) - \varphi_{LO}(t)$ are the central frequency and phase noise of the MMW signal, respectively.

Subsequently, this MMW signal is transmitted over a pair of horn antennas (HA), and then is down-converted to intermediate frequency (IF) through the electronic coherent mixing down-conversion (including an RF source and a MMW mixer). Finally, the obtained IF signal is processed in the receiving DSP after analog-to-digital conversion. Under small signal approximation, the obtained IF signal can be given as

$$E_{IF}(t) \propto \sin[2\pi f_{IF} t + \Delta\phi(t) + mu_1(t)]$$
$$+ \cos[2\pi f_{IF} t + \Delta\phi(t) + mu_2(t)]$$
$$\approx \cos[2\pi f_{IF} t + \Delta\phi(t)] + \sin[2\pi f_{IF} t + \Delta\phi(t)]$$
$$+ mu_1(t) \cdot \cos[2\pi f_{IF} t + \Delta\phi(t)]$$
$$- mu_2(t) \cdot \sin[2\pi f_{IF} t + \Delta\phi(t)] \qquad (5)$$

where f_{IF} and $\Delta\phi(t)$ represent the center frequency and overall phase noise of the down-converted IF signal, respectively. From (5), it can be seen that the first two terms are the IF carriers orthogonal to each other, and the last two terms are the desired information-bearing signals. It should be emphasized that the $u_1(t)$ and $u_2(t)$, which comprises two independent microwave vector signals, are carried by two orthogonal IF carriers with an overlapping spectrum, as shown in inset (c) of Fig. 1.

B. Signal Recovery DSP Approach for OFM Scheme

To simplify the system structure and reduce its cost, the LD and LO are preferred to use two free-running lasers. However, as mentioned in Section I, the generated MMW signal carries serious laser phase noise, which will also be transferred to the down-converted IF signal. At the receiving DSP side, to separate the $u_1(t)$ and $u_2(t)$ from the overlapping spectrum and meanwhile cancel the concomitant phase noise, a novel carrier extraction and signal recovery DSP approach is proposed, as shown in Fig. 2(a). It mainly includes two steps: the first is carrier extraction using Hilbert superposition, and the second is signal recovery based on the RFP phase noise cancellation. In step 1, the Hilbert transform is first performed on the obtained IF signal. Taking the positive frequency component as an example, the Hilbert transform operation means a phase shift by -90° is applied to the original signal, which can be given as

$$\hat{E}_{IF}(t) = \sin[2\pi f_{IF} t + \Delta\phi(t)] - \cos[2\pi f_{IF} t + \Delta\phi(t)]$$
$$+ mu_1(t) \cdot \sin[2\pi f_{IF} t + \Delta\phi(t)]$$
$$+ mu_2(t) \cdot \cos[2\pi f_{IF} t + \Delta\phi(t)] \qquad (6)$$

The sketch diagrams of obtained IF signal and its Hilbert transform form are shown in Fig. 2(a)(i) and (ii), respectively. Then the IF carrier in the cosine direction as shown in the inset (iii) of Fig. 2(a) can be extracted by Hilbert transform superposition

$$E_C(t) = BPF\left[E_{IF}(t) - \hat{E}_{IF}(t)\right] \propto \cos[2\pi f_{IF} t + \Delta\phi(t)] \qquad (7)$$

As long as the f_s is larger than the half bandwidth of the information-bearing signal (i.e, BW/2), then the IF carrier can be successfully separated from the sideband signal by the band-pass
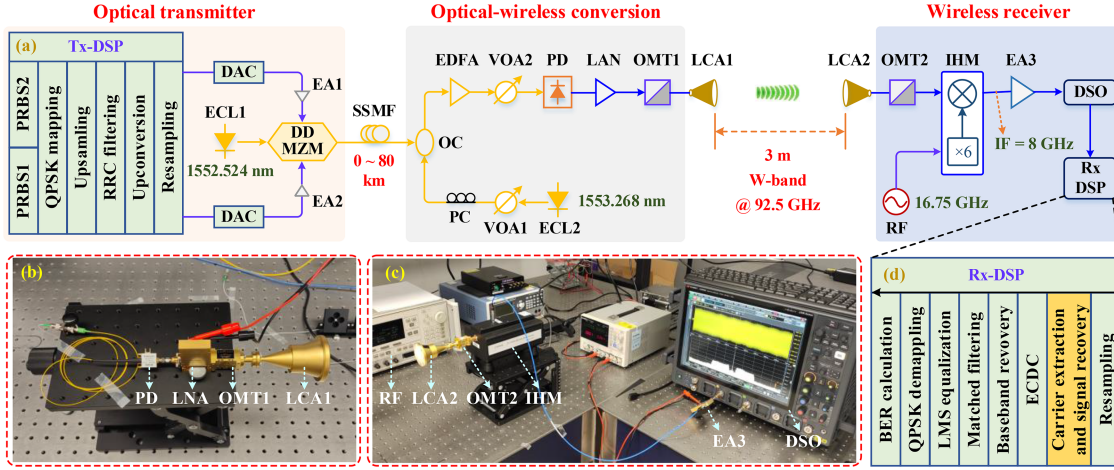
Fig. 3. Experimental setup for OFM transmission at W band with laser phase noise robustness enabled by a novel receiving DSP approach. (a) Transmitting DSP. (b) Photo of W-band transmitter in optical-wireless conversion side. (c) Photo of W-band wireless receiver. (d) Receiving DSP.

filtering. Up to now, the step 1 has already completed. In step 2, utilizing the phase orthogonality, the two desired signals, i.e., $u_1(t)$ and $u_2(t)$, can be recovered by RFP-based signal processing [3]

$$LPF\left[E_C(t) \times E_{IF}(t)\right] \propto u_1(t) \qquad (8)$$

$$LPF\left[E_C(t) \times \hat{E}_{IF}(t)\right] \propto u_2(t) \qquad (9)$$

where LPF represents the low-pass filter. It should be emphasized that the unstable offset frequency drift as well as the laser phase noise are all transferred to the high-frequency components after the multiplication between the carrier and signal, which are exactly removed by the LPF. In other words, the recovered $u_1(t)$ and $u_2(t)$ are robust to the phase noise resulting from the two free-running lasers in optical heterodyne detection. Moreover, it can be seen from Fig. 1 that only one analog transmission link is used, thus the residual phase noise can also be reduced, due to avoiding the path mismatch in hybrid fiber-wireless transmission links and phase imbalance in the optical coherent receiver.

However, it can be found from Fig. 2(a) (iv) and (v) that the recovered signals after step 2 are the superposition of the lower and upper sidebands (i.e., LSB and USB) of the original DSB signal. Therefore, the CD-induced power fading will undoubtedly be present in the fiber transmission scene, similar to the direct detection of DSB signal [30]. This is mainly because the two sideband signals have a frequency-dependent phase offset from the central carrier, which is caused by the CD effect of the fiber medium. Accordingly, the previous phase alignment state between the carrier and sideband signals in optical back-to-back case is destroyed by this additional phase offset. As a results, not only an intra frequency-dependent power fading for $u_1(t)$ or $u_2(t)$ during the superposition of LSB and USB [31], but also an unexpected inter crosstalk between the obtained $u_1(t)$ and $u_2(t)$ according to (8) and (9) are introduced. Fortunately, the electrical CD compensation (ECDC) based on the form of $u_1(t) + j \cdot u_2(t)$, which is well in accordance with the signal transmission form on the fiber according to (3), can effectively solve the above problems by correcting this phase mismatch.

After recovering $u_1(t)$ and $u_2(t)$, the transmitted two independent microwave vector signals, $s_1(t)$ and $s_2(t)$ can be acquired by $s_1(t) = u_1(t) - u_2(t)$ and $s_2(t) = u_1(t) + u_2(t)$, respectively. Finally, the real and imaginary parts of two independent complex baseband signals can be further demodulated through a digital coherent DSP according to (1) and (2).

For comparison with the proposed scheme, the conventional RFP phase noise cancellation scheme [4] for conventional DSB form (only transmitting one single DSB signal) is also shown in Fig. 2(b). At this case, the DDMZM is driven by a pair of inverting signals, i.e., $u_1(t) = s_1(t)$, $u_2(t) = -s_1(t)$. According to (5), the obtained IF signal for conventional DSB scheme can be expressed as

$$\begin{aligned} E'_{IF}(t) \approx &\cos\left[2\pi f_{IF}t + \Delta\phi(t)\right] + \sin\left[2\pi f_{IF}t + \Delta\phi(t)\right] \\ &+ ms_1(t) \cdot \cos\left[2\pi f_{IF}t + \Delta\phi(t)\right] \\ &+ ms_1(t) \cdot \sin\left[2\pi f_{IF}t + \Delta\phi(t)\right] \end{aligned} \qquad (10)$$

The inset (i) of Fig. 2(b) shows the sketch diagram of the above-obtained IF signal, in which $s_1(t)$ is simultaneously carried by the LSB and USB in both cosine and sine directions. Different from (7), the carrier can be extracted without Hilbert transform superposition, thus it can be given as

$$\begin{aligned} E'_C(t) &= BPF\left[E'_{IF}(t)\right] \\ &= \cos\left[2\pi f_{IF}t + \Delta\phi(t)\right] + \sin\left[2\pi f_{IF}t + \Delta\phi(t)\right] \end{aligned} \qquad (11)$$

Then the desired signal $s_1(t)$ can be recovered by

$$LPF\left[E'_C(t) \times E'_{IF}(t)\right] \propto s_1(t) \qquad (12)$$

From the above process, it can be found that the conventional RFP phase noise cancellation scheme directly extracts the IF carrier and then multiplies it with the original signal to recover the desired signal. As a result, this scheme only outputs one-dimensional information, it quite differs from the proposed scheme shown in Fig. 2(a) which outputs two-dimensional information in the orthogonal direction of phase. At this case, since
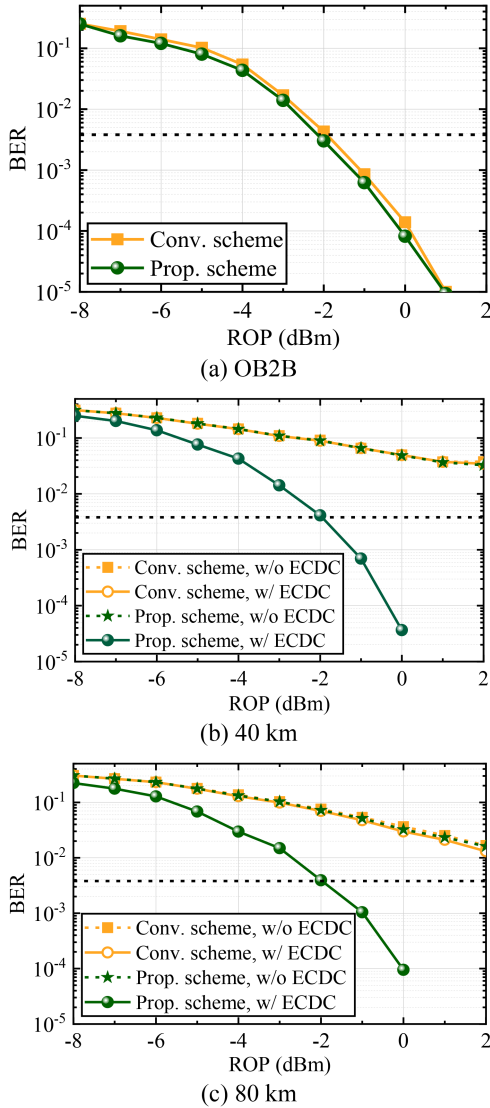
Fig. 4.   BER performance comparison with (w/) and without (w/o) ECDC for single 6-GBd DSB signal between conventional and proposed schemes over 3-m wireless and different fiber transmission distances. (a) OB2B. (b) 40 km. (c) 80 km.

the joint ECDC based on the two-dimensional information cannot be applied, the power fading phenomenon also remains after the superposition of LSB and USB (see inset (ii) of Fig. 2(b)) in the fiber transmission case. The detailed performance comparisons between the two schemes will be discussed in Section IV.

III. EXPERIMENTAL SETUP

Fig. 3 shows the experimental setup of our OFM-based photonics-assisted MMW communication link at W band using single DDMZM modulation and single-end PD detection. At the optical transmitter, two 3-GBd microwave vector QPSK signals with an identical carrier frequency of 2.15 GHz are first generated in the transmitting DSP, as shown in Fig. 3(a). To better demonstrate and verify the OFM transmission scheme, two sets of independent pseudo-random binary sequences with the same length of 2^{17} are adopted. Then they are mapped into

the QPSK symbols with different initial phases of 0° and 45° in our proof-of-concept experiment, respectively. After upsampled to 4 samples per symbol, the two sets of QPSK symbols are shaped by a root-raised-cosine (RRC) filter with a rolloff factor of 0.1. Subsequently, the up-conversion is conducted with a center frequency of $f_s = 2.15$ GHz, reserving a guard band of 0.5 GHz which is enough to extract the fluctuating IF carrier (a frequency drift within 300 MHz is observed due to the two free-running lasers). Accordingly, two independent microwave vector QPSK signals have been successfully generated, and then are fed to one 92-GSa/s arbitrary waveform generator after simple cross-processing as mentioned in Section II-B to avoid the power imbalance. A low-cost DDMZM is used to modulate the two QPSK signals on a single optical carrier. The input laser adopts one external cavity laser (ECL1) with the central wavelength of 1552.524 nm, output power of 10 dBm and linewidth of < 100 kHz. By biasing the DDMZM at its quadrature transmission point, the optical orthogonal modulation is achieved, which can present a spectrally efficient overlapping DSB transmission on a single optical wavelength with the form of $u_1(t) + j \cdot u_2(t)$.

After transmission over 0∼80-km SSMF, the modulated optical OFM signals are then coupled with an optical LO (i.e., ECL2) with the central wavelength of 1553.268 nm in the optical-wireless conversion side. The LO power is controlled at 0 dBm through a variable optical attenuator (VOA1), and one polarization controller (PC) is applied to align its polarization direction with that of the arrived signal lightwave. The frequency difference between the two lightwaves is set to 92.5 GHz. Next, the combined lightwaves are fed to a single-end PD with 3-dB bandwidth of 100 GHz and responsivity of 0.6 A/W after boosted by one erbium-doped fiber amplifier (EDFA). Utilizing the optical heterodyne detection, a W-band MMW signal with OFM located at 92.5 GHz can be generated. To adjust the receiving optical power (ROP) before photoelectric detection, another VOA (i.e., VOA2) is placed before the PD. Afterwards, the generated 92.5-GHz OFM MMW signal carrying two independent QPSK information is first amplified by a 75∼110-GHz low noise amplifier (LNA) with 35-dB gain, and then is fed to a W-band lens corrected antenna (LCA1) through an orthomode transducer (OMT1). After 3-m air transmission, the wireless signal is received by another LCA (i.e., LCA2). A pair of LCAs can offer a total gain of 2 × 30 dBi, hence the 83.1-dB air path loss for 92.5-GHz MMW transmission over 3-m wireless distance can be partially compensated. Noting that the two LCAs support simultaneous transmission of horizontal/vertical dual-polarized wireless signals, which can cooperate well with the optical PDM scheme to further improve the system spectral efficiency. However, only one polarization is used through OMT in our proof-of-concept experiment for brevity. Fig. 3(b) shows the photo of the W-band transmitter on the optical-wireless conversion side.

At the wireless receiver end, as shown in Fig. 3(c), the received 92.5-GHz OFM MMW signal is first fed to an integrated harmonic mixer (IHM) for electronic mixing down-conversion via another OMT (i.e., OMT2). The IHM consists of a frequency multiplier chain with six times and one mixer with a WR10 waveguide interface (75∼110 GHz). The input RF source is set
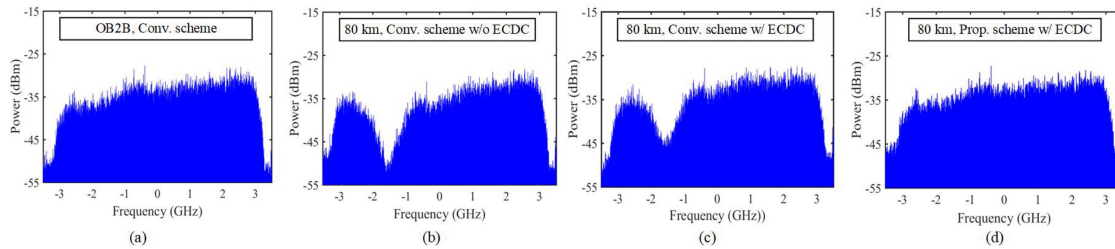
Fig. 5. The spectra of single 6-GBd DSB signal at a fixed ROP of 0 dBm after baseband recovery in the receiving DSP. (a) OB2B transmission case using conventional scheme. 80-km SSMF transmission case employing (b) conventional scheme without ECDC, (c) conventional scheme with ECDC and (d) proposed scheme with ECDC.

to 16.75 GHz with 6-dBm power, thus an IF signal with the center frequency of around 8 GHz (16.75 × 6 – 92.5) can be obtained after down-conversion. Subsequently, this IF signal is amplified by one electrical amplifier (EA) with a gain of 30 dB, and then is sampled via a 128-GSa/s digital storage oscilloscope (DSO) for offline DSP demodulation. The detailed DSP workflow is shown in Fig. 3(d). Firstly, the obtained OFM IF signals with overlapping DSB are resampled to 4 samples per symbol. Then the proposed carrier extraction and signal recovery approach as shown in Fig. 2(a) is used to separate the $u_1(t)$ and $u_2(t)$ from the overlapping DSB signals and meanwhile cancel the concomitant phase noise. Afterwards, as mentioned above, a joint ECDC based on the form of $u_1(t) + j \cdot u_2(t)$ can effectively compensate the intra power fading for $u_1(t)$ or $u_2(t)$ and inter crosstalk between $u_1(t)$ and $u_2(t)$. Thus the transmitted two independent QPSK signals, $s_1(t)$ and $s_2(t)$, can be accurately acquired from the corrected $u_1(t)$ and $u_2(t)$. Finally, two sets of identical DSP are used to further demodulate the two independent QPSK signals, including baseband recovery, matched filtering, down-sampling, least mean square (LMS) equalization, symbol demapping and bit error rate (BER) calculation. Note that no additional carrier phase estimation is used in our receiving DSP.

IV. RESULTS AND DISCUSSIONS

We first evaluate the impact of fiber CD on the transmitting DSB signal based on the proposed carrier extraction and signal recovery DSP approach in the above photonics-assisted MMW communication link. Since the inter spectrum superposition between the two independent DSB signals in the OFM transmission case is not conducive to exhibiting the CD impact, a single DSB transmission case is first considered and studied in our experiment. For this purpose, we set $s_2(t)$ to zero while retaining $s_1(t)$. That is, the DDMZM with the quadrature transmission point is driven by $u_1(t) = s_1(t)$ in the upper arm and $u_2(t) = -s_1(t)$ in the lower arm, thus a single commonly used DSB signal form can be successfully generated after electro-optic modulation. In addition to the proposed carrier extraction and signal recovery scheme as shown in Fig. 2(a) (termed as proposed scheme in the following), the conventional RFP phase noise cancellation scheme as shown in Fig. 2(b) (termed as conventional scheme) is also adopted in the receiving DSP for comparison. After setting $s_2(t) = 0$, there is now an inverse relationship between $u_1(t)$ and $u_2(t)$, i.e., $u_1(t) = -u_2(t)$. For conventional RFP scheme,

$s_1(t)$ can be recovered by the direct multiplication between the extracted carrier and signal. For the proposed scheme, the $u_1(t)$ and $u_2(t)$ can also be successfully recovered according to (8) and (9), respectively. Then the $s_1(t)$ can be obtained from either $u_1(t)$ or $u_2(t)$. Noting that in the case of optical back-to-back (OB2B), the phases of $u_1(t)$ and $u_2(t)$ well align with the carrier in their own directions as shown in the inset (i) of Fig. 2(a). However, after the fiber transmission, the CD-induced phase mismatch between the carrier and sideband signals leads to the $u_1(t)$ or $u_2(t)$ appearing in both two orthogonal directions with a complementary power. This may have a serious impact on traditional RFP scheme with only one-dimensional information output. Fig. 4 shows the corresponding BER performance of one single 6-GBd DSB QPSK signal for the abovementioned two receiving schemes over 3-m wireless and three kinds of different fiber transmission distances, including the OB2B, 40 km and 80 km cases. For the OB2B case as shown in Fig. 4(a), the two receiving schemes have similar performance, due to the absence of fiber CD. However, the BER performance of both schemes is deteriorated by the CD-induced power fading in the 40-km and 80-km SSMF transmission cases as shown in Fig. 4(b) and (c), respectively. Especially, for the conventional scheme, this power fading still cannot be compensated even if the ECDC is used. Instead, by adopting the joint ECDC based on the obtained two complementary components according to Fig. 2(a), our proposed scheme can successfully correct the phase mismatch and thus effectively compensate the frequency-dependent power fading. It can be seen from Fig. 4(b) and (c), after transmission over a 40-km or 80-km SSMF, the 6-GBd DSB signal can achieve similar performance to the OB2B case after ECDC. Fig. 5 gives the spectra of 6-GBd DSB signal at a fixed ROP of 0 dBm after baseband recovery in the receiving DSP. The recovered spectra in the OB2B and 80-km cases without ECDC for the conventional scheme are shown in Fig. 5(a) and (b). In comparison, an obvious frequency-dependent power fading phenomenon can be observed from Fig. 5(b). However, as shown in Fig. 5(c), the power fading phenomenon is still not effectively compensated even with ECDC for the conventional scheme. Fortunately, this power fading can be overcome by using our proposed scheme, the obtained spectrum after ECDC is shown in Fig. 5(d).

Given the above, we have demonstrated the immunity to the fiber CD when transmitting a single DSB signal. In fact, this proposed scheme is also suitable for the OFM case with overlapping DSB transmission. By using this proposed scheme,
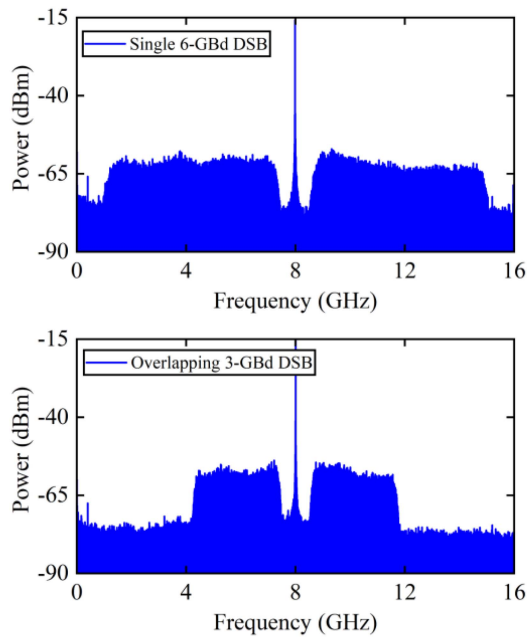
Fig. 6. Measured IF spectra after down-conversion for (a) single 6-GBd DSB and (b) two 3-GBd overlapping DSB transmission cases.
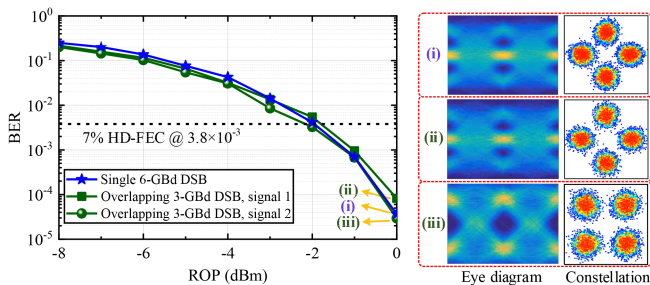

Fig. 7. BER versus ROP curves for the two different transmission schemes over 3-m wireless and 40-km SSMF link. Insets (i) ∼ (iii) show the corresponding eye diagrams and constellation diagrams at a fixed ROP of 0 dBm.

we further give the performance comparison between one single 6-GBd DSB and two 3-GBd overlapping DSB QPSK signals transmission over 40-km fiber and 3-m wireless. Fig. 6 shows their corresponding IF spectra after down-conversion. Note that two independent QPSK signals are completely overlapped in the frequency domain for the overlapping DSB case as shown in Fig. 6(b). It can achieve the same transmission rate as that of the single 6-GBd DSB case as shown in Fig. 6(a), but the bandwidth is halved. Fig. 7 shows the BER versus ROP curves for the above two cases. It can be found that the proposed OFM scheme with overlapping DSB transmission presents a similar performance as that of the single 6-GBd DSB case. For instance, both two cases can reach the BER threshold (3.8×10^{-3}) of 7% overhead hard-decision forward error correction (HD-FEC) at a ROP of around −2 dBm. The corresponding eye diagrams and constellation diagrams at the ROP of 0 dBm for single 6-GBd DSB and two 3-GBd overlapping DSB QPSK signals are given in insets (i) ∼ (iii) of Fig. 7. According to insets (i) and (ii), we can also observe an approximate performance. Therefore, the

proposed photonics-assisted MMW communication link using the OFM transmission scheme can double the spectral efficiency in both the optical and electrical links, as compared with the conventional DSB transmission scheme. Moreover, from the distribution of constellation points in the three constellation diagrams, it can be inferred that there is almost no obvious residual phase noise. This means the laser phase noise robustness has also been successfully achieved in our proposed scheme.

V. CONCLUSION

To summarize, we have proposed a simple photonics-assisted MMW communication link using an OFM transmission scheme. The OFM is achieved by single DDMZM modulation and single-end PD detection, and it can support the simultaneous transmission of two independent DSB signals with an identical carrier frequency. A novel DSP approach is also proposed, which can not only separate the two independent DSB signals from an overlapping spectrum, but also overcome the CD-induced power fading and the laser phase noise resulting from two free-running lasers. The proposed scheme is verified via a proof-of-concept experiment. Two independent QPSK signals based on the OFM scheme are simultaneously transmitted over up to 80-km fiber and 3-m wireless at W band. The experimental results show that the proposed DSP approach can successfully recover the two independent QPSK signals without using any extra carrier phase estimation algorithm. In addition, our proposed scheme can achieve twice of the spectral efficiency for fiber-MMW hybrid communication links as compared with the conventional DSB transmission scheme. More importantly, if this OFM scheme in conjunction with the PDM technique, the system spectral efficiency can be further improved. Thus, it may become a potential low-cost, low-power access solution for photonics-assisted MMW communication links in the upcoming B5G and 6G networks.

REFERENCES

[1] J. Yu, "Photonics-assisted millimeter-wave wireless communication," *IEEE J. Quantum Electron.*, vol. 53, no. 6, Dec. 2017, Art. no. 8000517.
[2] X. Li, J. Yu, and G.-K. Chang, "Photonics-aided millimeter-wave technologies for extreme mobile broadband communications in 5G," *J. Lightw. Technol.*, vol. 38, no. 2, pp. 366–378, Jan. 2020.
[3] M. Zhu et al., "Ultra-wideband fiber-THz-fiber seamless integration communication system toward 6G: Architecture, key techniques, and testbed implementation," *Sci. China Inf. Sci.*, vol. 66, no. 1, Jan. 2023, Art. no. 113301.
[4] Y. Cai, X. Gao, Y. Ling, B. Xu, and K. Qiu, "RF pilot tone phase noise cancellation based on DD-MZM SSB modulation for optical heterodyne RoF link," *Opt. Commun.*, vol. 454, 2020, Art. no. 124502.
[5] L. Giorgi et al., "Subcarrier multiplexing RF plans for analog radio over fiber in heterogeneous networks," *J. Lightw. Technol.*, vol. 34, no. 16, pp. 3859–3866, Aug. 2016.
[6] P. T. Dat, A. Kanno, N. Yamamoto, N. Van Dien, N. T. Hung, and T. Kawanishi, "Full-duplex transmission of Nyquist-SCM signal over a seamless bidirectional fiber–wireless system in W-band," in *Proc. Opt. Fiber Commun. Conf.*, 2019, pp. 1–3.
[7] C. Liu et al., "Non-orthogonal multiple access based on SCMA and OFDM/OQAM techniques in bidirectional RoF system," in *Proc. Opt. Fiber Commun. Conf. Exhib.*, 2017, pp. 1–3.
[8] D.-N. Nguyen et al., "Polarization division multiplexing-based hybrid microwave photonic links for simultaneous mmW and sub-6 GHz wireless transmissions," *IEEE Photon. J.*, vol. 12, no. 6, Dec. 2020, Art. no. 5502814.

[9] H. Zhang, A. Wen, W. Zhang, W. Zhang, and Z. Tu, "A spectral-efficient self-homodyne-detected microwave photonic link with an extended fiber-reach," *IEEE Photon. Technol. Lett.*, vol. 30, no. 19, pp. 1719–1722, Oct. 2018.

[10] J.-H. Yan, J.-K. Huang, Y.-Y. Lin, J.-W. Hsu, and K.-M. Feng, "A MMW coordinate multi-point transmission system for 5G mobile fronthaul networks based on a polarization-tracking-free PDM-RoF mechanism," in *Proc. Opt. Fiber Commun. Conf.*, 2020, pp. 1–3.

[11] P. T. Dat, F. Rottenberg, A. Kanno, N. Yamamoto, and T. Kawanishi, "3 × 3 MIMO fiber–Wireless system in W-band with WDM/PDM RoF transmission capability," *J. Lightw. Technol.*, vol. 39, no. 24, pp. 7794–7803, Dec. 2021.

[12] F. Li, Z. Cao, X. Li, Z. Dong, and L. Chen, "Fiber-wireless transmission system of PDM-MIMO-OFDM at 100 GHz frequency," *J. Lightw. Technol.*, vol. 31, no. 14, pp. 2394–2399, Jul. 2013.

[13] Y. Chen, J. Xiao, and Z. Dong, "Delivering dual polarization-division-multiplexing millimeter-wave signals at W-band by one pair of antennas," *IEEE Photon. J.*, vol. 11, no. 5, Oct. 2019, Art. no. 6602710.

[14] Y. Cai et al., "Real-time 100-GbE fiber-wireless seamless integration system using an electromagnetic dual-polarized single-input single-output wireless link at W band," *Opt. Lett.*, vol. 48, no. 4, pp. 928–931, Feb. 2023.

[15] J. Zhang, J. Yu, N. Chi, Z. Dong, X. Li, and G.-K. Chang, "Multichannel 120-Gb/s data transmission over 2×2 MIMO fiber-wireless link at W-band," *IEEE Photon. Technol. Lett.*, vol. 25, no. 8, pp. 780–783, Apr. 2013.

[16] J. Zhang et al., "Real-time demonstration of 103.125-Gbps fiber–THz–fiber 2 × 2 MIMO transparent transmission at 360–430 GHz based on photonics," *Opt. Lett.*, vol. 47, no. 5, pp. 1214–1217, Mar. 2022.

[17] Y. Chen, T. Shao, A. Wen, and J. Yao, "Microwave vector signal transmission over an optical fiber based on IQ modulation and coherent detection," *Opt. Lett.*, vol. 39, no. 6, pp. 1509–1512, Mar. 2014.

[18] X. Chen and J. Yao, "A high spectral efficiency coherent microwave photonic link employing both amplitude and phase modulation with digital phase noise cancellation," *J. Lightw. Technol.*, vol. 33, no. 14, pp. 3091–3097, Jul. 2015.

[19] P. Li, R. Xu, Z. Dai, Z. Lu, L. Yan, and J. Yao, "A high spectral efficiency radio over fiber link based on coherent detection and digital phase noise cancellation," *J. Lightw. Technol.*, vol. 39, no. 20, pp. 6443–6449, Oct. 2021.

[20] P. Li, Z. Dai, L. Yan, and J. Yao, "Microwave photonic link to transmit four microwave vector signals on a single optical carrier based on coherent detection and digital signal processing," *Opt. Exp.*, vol. 30, no. 5, pp. 6690–6699, Oct. 2022.

[21] X. Chen and J. Yao, "Data rate quadrupled coherent microwave photonic link," *IEEE Photon. Technol. Lett.*, vol. 29, no. 13, pp. 1071–1074, Jul. 2017.

[22] Y. Cai et al., "Large-capacity photonics-assisted millimeter-wave wireless communication enabled by dual-polarized SISO link and advanced MIMO equalizer," *J. Lightw. Technol.*, vol. 42, no. 11, pp. 4048–4059, Jun. 2024, doi: 10.1109/JLT.2024.3384379.

[23] M. S. Faruk and K. Kikuchi, "Compensation for in-phase/quadrature imbalance in coherent-receiver front end for optical quadrature amplitude modulation," *IEEE Photon. J.*, vol. 5, no. 2, Apr. 2013, Art. no. 7800110.

[24] W.-R. Peng, T. Tsuritani, and I. Morita, "Simple carrier recovery approach for RF-pilot-assisted PDM-CO-OFDM systems," *J. Lightw. Technol.*, vol. 31, no. 15, pp. 2555–2564, Aug. 2013.

[25] Y. Zou et al., "Two independent microwave vector signals transmission based on single DDMZM modulation at W band," in *Proc. Opto-Electron. Commun. Conf.*, 2023, pp. 1–3.

[26] Y. Cai, X. Gao, Y. Ling, B. Xu, and K. Qiu, "Performance comparison of optical single-sideband modulation in RoF link," *Opt. Commun.*, vol. 463, Art. no. 125409, May 2013.

[27] Q. Zhang, N. Stojanovic, C. Xie, C. Prodaniuc, and P. Laskowski, "Transmission of single lane 128 Gbit/s PAM-4 signals over an 80 km SSMF link, enabled by DDMZM aided dispersion pre-compensation," *Opt. Exp.*, vol. 24, no. 21, pp. 24580–24591, 2016.

[28] K.-P. Ho and H.-W. Cuei, "Generation of arbitrary quadrature signals using one dual-drive modulator," *J. Lightw. Technol.*, vol. 23, no. 2, pp. 764–770, Feb. 2005.

[29] W. Wang, F. Li, Z. Li, Q. Sui, and Z. Li, "Dual-drive Mach-Zehnder modulator-based single side-band modulation direct detection system without signal-to-signal beating interference," *J. Lightw. Technol.*, vol. 38, no. 16, pp. 4341–4351, Aug. 2020.

[30] B. Lin, J. Li, H. Yang, Y. Wan, Y. He, and Z. Chen, "Comparison of DSB and SSB transmission for OFDM-PON," *J. Opt. Commun. Netw.*, vol. 4, no. 11, pp. B94–B100, Nov. 2012.

[31] Y. Gao, A. Wen, Y. Chen, S. Xiang, H. Zhang, and L. Shang, "An analog photonic link with compensation of dispersion-induced power fading," *IEEE Photon. Technol. Lett.*, vol. 27, no. 12, pp. 1301–1304, Jun. 2015.